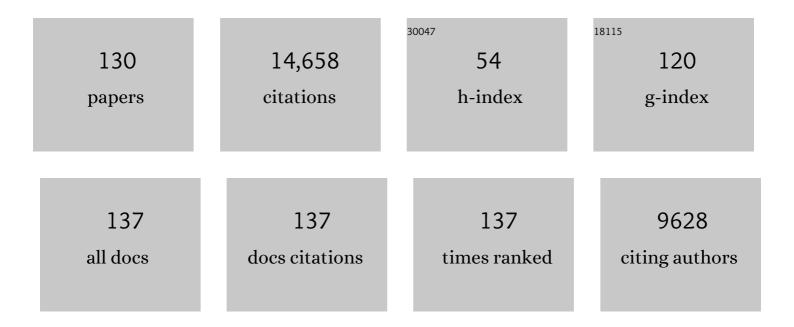
List of Publications by Year in descending order

Source: https://exaly.com/author-pdf/1521700/publications.pdf Version: 2024-02-01



#	Article	lF	CITATIONS
1	Valence bond description of antiferromagnetic coupling in transition metal dimers. Journal of Chemical Physics, 1981, 74, 5737-5743.	1.2	2,333
2	Copper(I)-Catalyzed Synthesis of Azoles. DFT Study Predicts Unprecedented Reactivity and Intermediates. Journal of the American Chemical Society, 2005, 127, 210-216.	6.6	1,497
3	Ligand spin polarization and antiferromagnetic coupling in transition metal dimers. Chemical Physics, 1986, 109, 131-143.	0.9	904
4	Orbital interactions, electron delocalization and spin coupling in iron-sulfur clusters. Coordination Chemistry Reviews, 1995, 144, 199-244.	9.5	758
5	Density-Functional Theory of Spin Polarization and Spin Coupling in Iron—Sulfur Clusters. Advances in Inorganic Chemistry, 1992, 38, 423-470.	0.4	570
6	Electronic structure, magnetic properties, ESR, and optical spectra for 2-iron ferredoxin models by LCAO-X.alpha. valence bond theory. Journal of the American Chemical Society, 1984, 106, 2316-2327.	6.6	517
7	The Xα valence bond theory of weak electronic coupling. Application to the lowâ€lying states of Mo2Cl84â^'. Journal of Chemical Physics, 1979, 70, 4903-4906.	1.2	397
8	Quantum Chemical Studies of Intermediates and Reaction Pathways in Selected Enzymes and Catalytic Synthetic Systems. Chemical Reviews, 2004, 104, 459-508.	23.0	365
9	Why Is Tetrazole Formation by Addition of Azide to Organic Nitriles Catalyzed by Zinc(II) Salts?. Journal of the American Chemical Society, 2003, 125, 9983-9987.	6.6	333
10	Density Functional/Poisson-Boltzmann Calculations of Redox Potentials for Iron-Sulfur Clusters. Journal of the American Chemical Society, 1994, 116, 11898-11914.	6.6	305
11	Mechanisms of Tetrazole Formation by Addition of Azide to Nitriles. Journal of the American Chemical Society, 2002, 124, 12210-12216.	6.6	303
12	Models for ferredoxins: electronic structures of iron-sulfur clusters with one, two, and four iron atoms. Journal of the American Chemical Society, 1985, 107, 3418-3426.	6.6	288
13	Calculation of Redox Potentials and pKa Values of Hydrated Transition Metal Cations by a Combined Density Functional and Continuum Dielectric Theory. Inorganic Chemistry, 1996, 35, 4694-4702.	1.9	238
14	Broken symmetry analysis of spin coupling in iron-sulfur clusters. Journal of the American Chemical Society, 1988, 110, 1001-1005.	6.6	225
15	Density Functional and Reduction Potential Calculations of Fe4S4Clusters. Journal of the American Chemical Society, 2003, 125, 1923-1936.	6.6	220
16	Calculating the Electron Paramagnetic Resonance Parameters of Exchange Coupled Transition Metal Complexes Using Broken Symmetry Density Functional Theory:Â Application to a MnIII/MnIVModel Compound. Journal of the American Chemical Society, 2004, 126, 2613-2622.	6.6	194
17	FeMo Cofactor of Nitrogenase:Â A Density Functional Study of States MN, MOX, MR, and MI. Journal of the American Chemical Society, 2001, 123, 12392-12410.	6.6	181
18	Incorporating Solvation Effects into Density Functional Electronic Structure Calculations. The Journal of Physical Chemistry, 1994, 98, 11059-11068.	2.9	171

#	Article	IF	CITATIONS
19	Structural, Spectroscopic, and Redox Consequences of a Central Ligand in the FeMoco of Nitrogenase:  A Density Functional Theoretical Study. Journal of the American Chemical Society, 2003, 125, 8377-8383.	6.6	146
20	Spin Densities and Spin Coupling in Iron-Sulfur Clusters: A New Analysis of Hyperfine Coupling Constants. Inorganic Chemistry, 1995, 34, 4347-4359.	1.9	145
21	Density Functional Study of the Valence-Tautomeric Interconversion Low-Spin [Colll(SQ)(Cat)(phen)] ⇌ High-Spin [Coll(SQ)2(phen)]. Inorganic Chemistry, 1997, 36, 3966-3984.	1.9	142
22	Incorporating Protein Environments in Density Functional Theory:Â A Self-Consistent Reaction Field Calculation of Redox Potentials of [2Fe2S] Clusters in Ferredoxin and Phthalate Dioxygenase Reductase. Journal of Physical Chemistry A, 1998, 102, 6311-6324.	1.1	130
23	Insights into properties and energetics of iron–sulfur proteins from simple clusters to nitrogenase. Current Opinion in Chemical Biology, 2002, 6, 259-273.	2.8	127
24	A model for the spin states of high-potential iron-sulfur [Fe4S4]3+ proteins. Inorganic Chemistry, 1988, 27, 3677-3679.	1.9	122
25	Density functional calculation of pK a values and redox potentials in the bovine Rieske iron-sulfur protein. Journal of Biological Inorganic Chemistry, 2002, 7, 632-639.	1.1	117
26	Electronic structure of 2-Fe ferredoxin models by X.alpha. valence bond theory. Journal of the American Chemical Society, 1980, 102, 4279-4282.	6.6	105
27	Density Functional Calculations of Electronic Structure, Charge Distribution, and Spin Coupling in Manganeseâ°'Oxo Dimer Complexes. Inorganic Chemistry, 1997, 36, 1198-1217.	1.9	99
28	Exchange coupling and resonance delocalization in reduced iron-sulfur [Fe4S4]+ and iron-selenium [Fe4Se4]+ clusters. 1. Basic theory of spin-state energies and EPR and hyperfine properties. Inorganic Chemistry, 1991, 30, 246-256.	1.9	90
29	Density Functional Study on the Electronic Structures of Model Peroxidase Compounds I and II. Journal of the American Chemical Society, 1997, 119, 11442-11451.	6.6	90
30	CuZn Superoxide Dismutase Geometry Optimization, Energetics, and Redox Potential Calculations by Density Functional and Electrostatic Methods. Inorganic Chemistry, 1999, 38, 940-950.	1.9	90
31	Structure, redox, pK a, spin. A golden tetrad for understanding metalloenzyme energetics and reaction pathways. Journal of Biological Inorganic Chemistry, 2006, 11, 674-694.	1.1	89
32	Testing if the Interstitial Atom, X , of the Nitrogenase Molybdenumâ^'Iron Cofactor Is N or C: ENDOR, ESEEM, and DFT Studies of the <i>S</i> = ³ / ₂ Resting State in Multiple Environments. Inorganic Chemistry, 2007, 46, 11437-11449.	1.9	89
33	Sulfur [¹⁸ F]Fluoride Exchange Click Chemistry Enabled Ultrafast Late-Stage Radiosynthesis. Journal of the American Chemical Society, 2021, 143, 3753-3763.	6.6	89
34	A Fluorogenic Aryl Fluorosulfate for Intraorganellar Transthyretin Imaging in Living Cells and in <i>Caenorhabditis elegans</i> . Journal of the American Chemical Society, 2015, 137, 7404-7414.	6.6	86
35	A Theoretical Study of the UV/Visible Absorption and Emission Solvatochromic Properties of Solvent-Sensitive Dyes. ChemPhysChem, 2003, 4, 1084-1094.	1.0	84
36	A Structural Model for the High-Valent Intermediate Q of Methane Monooxygenase from Broken-Symmetry Density Functional and Electrostatics Calculations. Journal of the American Chemical Society, 2002, 124, 5890-5894.	6.6	83

#	Article	IF	CITATIONS
37	Density Functional Studies of the Ground- and Excited-State Potential-Energy Curves of Stilbenecis-trans Isomerization. ChemPhysChem, 2002, 3, 167-178.	1.0	75
38	Symmetry and Bonding in Metalloporphyrins. A Modern Implementation for the Bonding Analyses of Five- and Six-Coordinate High-Spin Iron(III)â~Porphyrin Complexes through Density Functional Calculation and NMR Spectroscopy. Journal of the American Chemical Society, 2003, 125, 6774-6783.	6.6	74
39	Exchange coupling and resonance delocalization in reduced iron-sulfur [Fe4S4]+ and iron-selenium [Fe4Se4]+ clusters. 2. A generalized nonlinear model for spin-state energies and EPR and hyperfine properties. Inorganic Chemistry, 1991, 30, 256-264.	1.9	72
40	Density Functional and Electrostatic Calculations of Manganese Superoxide Dismutase Active Site Complexes in Protein Environments. Inorganic Chemistry, 1999, 38, 929-939.	1.9	72
41	Nornicotine Aqueous Aldol Reactions:Â Synthetic and Theoretical Investigations into the Origins of Catalysis. Journal of Organic Chemistry, 2004, 69, 6603-6609.	1.7	72
42	Active Site Structure of Class I Ribonucleotide Reductase Intermediate X:Â A Density Functional Theory Analysis of Structure, Energetics, and Spectroscopy. Journal of the American Chemical Society, 2005, 127, 15778-15790.	6.6	70
43	Calibration of DFT Functionals for the Prediction of 57Fe Mössbauer Spectral Parameters in Iron–Nitrosyl and Iron–Sulfur Complexes: Accurate Geometries Prove Essential. Journal of Chemical Theory and Computation, 2011, 7, 3232-3247.	2.3	70
44	Modeling of palmitate transport in the heart. Molecular and Cellular Biochemistry, 1989, 88, 51-58.	1.4	69
45	Coupled Redox Potentials in Manganese and Iron Superoxide Dismutases from Reaction Kinetics and Density Functional/Electrostatics Calculations. Inorganic Chemistry, 2002, 41, 205-218.	1.9	69
46	Symmetry breaking and ionization from symmetry equivalent inner shells and lone pairs in Xα theory. Chemical Physics, 1982, 64, 159-166.	0.9	64
47	Toward a Chemical Mechanism of Proton Pumping by the B-Type Cytochrome <i>c</i> Oxidases: Application of Density Functional Theory to Cytochrome <i>ba</i> _{<i>3</i>} of <i>Thermus thermophilus</i> . Journal of the American Chemical Society, 2008, 130, 15002-15021.	6.6	63
48	DFT calculations of57Fe Mössbauer isomer shifts and quadrupole splittings for iron complexes in polar dielectric media: Applications to methane monooxygenase and ribonucleotide reductase. Journal of Computational Chemistry, 2006, 27, 1292-1306.	1.5	61
49	Structural model studies for the high-valent intermediate Q of methane monooxygenase from broken-symmetry density functional calculations. Inorganica Chimica Acta, 2008, 361, 973-986.	1.2	61
50	Valence electron delocalization in polynuclear iron-sulfur clusters. Journal of Biological Inorganic Chemistry, 1996, 1, 177-182.	1.1	60
51	Density Functional Theory Calculations on Mössbauer Parameters of Nonheme Iron Nitrosyls. Inorganic Chemistry, 2009, 48, 9155-9165.	1.9	60
52	Magnetic studies of the high-potential protein model [Fe4S4(S-2,4,6-(iso-Pr)3C6H2)4]- in the [Fe4S4]3+ oxidized state. Inorganic Chemistry, 1990, 29, 4288-4292.	1.9	58
53	Structural Model Studies for the Peroxo Intermediate P and the Reaction Pathway from P → Q of Methane Monooxygenase Using Broken-Symmetry Density Functional Calculations. Inorganic Chemistry, 2008, 47, 2975-2986.	1.9	58
54	The determination of optical absorption intensities using the Xα scattered wave method. Journal of Chemical Physics, 1976, 64, 2343.	1.2	57

#	Article	IF	CITATIONS
55	Selective naked-cluster cryophotochemistry and SCF-X.alphaSW calculations for copper (Cu2) and silver (Ag2). Journal of the American Chemical Society, 1979, 101, 3504-3511.	6.6	57
56	Analysis of the 57Fe Hyperfine Coupling Constants and Spin States in Nitrogenase P-Clusters. Inorganic Chemistry, 1994, 33, 4819-4830.	1.9	57
57	Ligand-Bound <i>S</i> = ¹ / ₂ FeMo-Cofactor of Nitrogenase: Hyperfine Interaction Analysis and Implication for the Central Ligand X Identity. Inorganic Chemistry, 2008, 47, 6162-6172.	1.9	57
58	Photoisomerization and Proton Transfer in Photoactive Yellow Protein. Journal of the American Chemical Society, 2003, 125, 8186-8194.	6.6	54
59	LCAO X.alpha. calculation of the magnetic exchange interactions in a manganese MnIVMn3III cubane complex: relevance to the water oxidation center of photosystem II. Journal of the American Chemical Society, 1992, 114, 6109-6119.	6.6	53
60	Metal Substitution in the Active Site of Nitrogenase MFe7S9(M = Mo4+, V3+, Fe3+). Inorganic Chemistry, 2002, 41, 5744-5753.	1.9	53
61	Density-Functional and Electrostatic Calculations for a Model of a Manganese Superoxide Dismutase Active Site in Aqueous Solution. The Journal of Physical Chemistry, 1996, 100, 13498-13505.	2.9	47
62	FeMo cofactor of nitrogenase: energetics and local interactions in the protein environment. Journal of Biological Inorganic Chemistry, 2002, 7, 735-749.	1.1	47
63	DFT Calculations of Isomer Shifts and Quadrupole Splitting Parameters in Synthetic Ironâ^'Oxo Complexes:  Applications to Methane Monooxygenase and Ribonucleotide Reductase. Inorganic Chemistry, 2003, 42, 5244-5251.	1.9	47
64	Binding Modes for the First Coupled Electron and Proton Addition to FeMoco of Nitrogenase. Journal of the American Chemical Society, 2002, 124, 4546-4547.	6.6	46
65	Density Functional Vertical Self-Consistent Reaction Field Theory for Solvatochromism Studies of Solvent-Sensitive Dyes. Journal of Physical Chemistry A, 2004, 108, 3545-3555.	1.1	45
66	Density Functional Study of the Mechanism of a Tyrosine Phosphatase:Â I. Intermediate Formation. Journal of the American Chemical Society, 2002, 124, 10225-10235.	6.6	44
67	Relative Acidities of Ortho-Substituted Phenols, as Models for Modified Tyrosines in Proteins. Journal of Physical Chemistry A, 2002, 106, 8757-8761.	1.1	41
68	A Density Functional Evaluation of an Fe(III)â^'Fe(IV) Model Diiron Cluster:Â Comparisons with Ribonucleotide Reductase Intermediate X. Inorganic Chemistry, 2003, 42, 2751-2758.	1.9	41
69	Linking Chemical Electron–Proton Transfer to Proton Pumping in Cytochrome <i>c</i> Oxidase: Broken-Symmetry DFT Exploration of Intermediates along the Catalytic Reaction Pathway of the Iron–Copper Dinuclear Complex. Inorganic Chemistry, 2014, 53, 6458-6472.	1.9	38
70	Broken symmetry effects in the He(I) valence photoelectron spectrum of Se(CN)2. Molecular Physics, 1982, 46, 609-620.	0.8	37
71	Theoretical Examination of Mg2+-Mediated Hydrolysis of a Phosphodiester Linkage as Proposed for the Hammerhead Ribozyme. Journal of the American Chemical Society, 2003, 125, 9861-9867.	6.6	37
72	Density-functional calculations of spin coupling in [Fe4S4]3+ clusters. International Journal of Quantum Chemistry, 1995, 56, 95-102.	1.0	36

#	Article	IF	CITATIONS
73	Density Functional Theory Study of the Intramolecular [2 + 3] Cycloaddition of Azide to Nitriles. Journal of Organic Chemistry, 2003, 68, 9076-9080.	1.7	36
74	Density Functional Studies of Oxidized and Reduced Methane Monooxygenase. Optimized Geometries and Exchange Coupling of Active Site Clusters. Inorganic Chemistry, 2001, 40, 5251-5266.	1.9	33
75	A study of the core electron binding energies of ozone by x-ray photoelectron spectroscopy and the Xα scattered wave method. Chemical Physics Letters, 1977, 49, 213-217.	1.2	32
76	Spin Coupling in Roussin's Red and Black Salts. Chemistry - A European Journal, 2010, 16, 10397-10408.	1.7	32
77	Density Functional Theory Analysis of Structure, Energetics, and Spectroscopy for the Mnâ^'Fe Active Site of <i>Chlamydia trachomatis</i> Ribonucleotide Reductase in Four Oxidation States. Inorganic Chemistry, 2010, 49, 7266-7281.	1.9	32
78	Geometric and Electrostatic Study of the [4Fe-4S] Cluster of Adenosine-5′-Phosphosulfate Reductase from Broken Symmetry Density Functional Calculations and Extended X-ray Absorption Fine Structure Spectroscopy. Inorganic Chemistry, 2011, 50, 6610-6625.	1.9	30
79	Using antibodies to perturb the coordination sphere of a transition metal complex. Nature, 1996, 382, 339-341.	13.7	29
80	Density Functional Theory Study of Fe(IV) dâ^'d Optical Transitions in Active-Site Models of Class I Ribonucleotide Reductase Intermediate X with Vertical Self-Consistent Reaction Field Methods. Inorganic Chemistry, 2006, 45, 8533-8542.	1.9	29
81	Seven clues to the origin and structure of class-I ribonucleotide reductase intermediate X. Journal of Inorganic Biochemistry, 2006, 100, 771-779.	1.5	29
82	Characterization of [4Fe-4Se]2+/3+ high-potential iron-sulfur protein from Chromatium vinosum. Biochemistry, 1988, 27, 8712-8719.	1.2	28
83	Energetics of Oxidized and Reduced Methane Monooxygenase Active Site Clusters in the Protein Environment. Inorganic Chemistry, 2001, 40, 5267-5278.	1.9	28
84	DFT calculations of comparative energetics and ENDOR/Mössbauer properties for two protonation states of the iron dimer cluster of ribonucleotide reductase intermediate X. Dalton Transactions, 2009, , 6045.	1.6	27
85	DFT Calculations for Intermediate and Active States of the Diiron Center with a Tryptophan or Tyrosine Radical in <i>Escherichia coli</i> Ribonucleotide Reductase. Inorganic Chemistry, 2011, 50, 2302-2320.	1.9	26
86	Density Functional Study of a μ-1,1-Carboxylate Bridged Fe(III)â^'Oâ^'Fe(IV) Model Complex. 2. Comparison with Ribonucleotide Reductase Intermediate X. Inorganic Chemistry, 2004, 43, 613-621.	1.9	25
87	Experimental and DFT Studies:Â Novel Structural Modifications Greatly Enhance the Solvent Sensitivity of Live Cell Imaging Dyes. Journal of Physical Chemistry A, 2007, 111, 10849-10860.	1.1	25
88	Quantum cluster size and solvent polarity effects on the geometries and Mössbauer properties of the active site model for ribonucleotide reductase intermediate X: a density functional theory study. Theoretical Chemistry Accounts, 2010, 125, 305-317.	0.5	23
89	Trimethylamine, trisilylamine, and trigermylamine: a comparative study of ionization energies, charge distribution, and bonding. Inorganic Chemistry, 1979, 18, 354-360.	1.9	22
90	On the Role of the Conserved Aspartate in the Hydrolysis of the Phosphocysteine Intermediate of the Low Molecular Weight Tyrosine Phosphatase. Journal of the American Chemical Society, 2004, 126, 12677-12684.	6.6	22

#	Article	IF	CITATIONS
91	The circumsphere as a tool to assess distortion in [4Fe-4S] atom clusters. Journal of Biological Inorganic Chemistry, 2003, 8, 519-526.	1.1	21
92	Density Functional Study for the Bridged Dinuclear Center Based on a High-Resolution X-ray Crystal Structure of <i>ba</i> ₃ Cytochrome <i>c</i> Oxidase from Thermus thermophilus. Inorganic Chemistry, 2013, 52, 14072-14088.	1.9	21
93	Use of Broken-Symmetry Density Functional Theory To Characterize the IspH Oxidized State: Implications for IspH Mechanism and Inhibition. Journal of Chemical Theory and Computation, 2014, 10, 3871-3884.	2.3	21
94	Broken Symmetry DFT Calculations/Analysis for Oxidized and Reduced Dinuclear Center in Cytochrome <i>c</i> Oxidase: Relating Structures, Protonation States, Energies, and Mössbauer Properties in <i>ba</i> ₃ <i>Thermus thermophilus</i> . Inorganic Chemistry, 2015, 54, 7272-7290.	1.9	21
95	A broken-symmetry density functional study of structures, energies, and protonation states along the catalytic O–O bond cleavage pathway in ba3 cytochrome c oxidase from Thermus thermophilus. Physical Chemistry Chemical Physics, 2016, 18, 21162-21171.	1.3	21
96	The electronic structure of tetraphosphorus trisulphide. Canadian Journal of Chemistry, 1977, 55, 669-681.	0.6	19
97	Broken-Symmetry DFT Computations for the Reaction Pathway of IspH, an Iron–Sulfur Enzyme in Pathogenic Bacteria. Inorganic Chemistry, 2015, 54, 6439-6461.	1.9	18
98	Modeling the MoFe Nitrogenase System with Broken Symmetry Density Functional Theory. Methods in Molecular Biology, 2011, 766, 293-312.	0.4	16
99	Water exit pathways and proton pumping mechanism in B-type cytochrome c oxidase from molecular dynamics simulations. Biochimica Et Biophysica Acta - Bioenergetics, 2016, 1857, 1594-1606.	0.5	15
100	X.alpha. scattered-wave calculations of the electronic structures of sulfur dioxide and sulfuryl fluoride. Relationship to .pi. bonding in the cyclic phosphazenes. Inorganic Chemistry, 1978, 17, 2709-2717.	1.9	14
101	Electronic structure in broken space- and spin- symmetry : applications to Fe-s proteins and clusters. Journal De Chimie Physique Et De Physico-Chimie Biologique, 1989, 86, 743-755.	0.2	14
102	Data for molecular dynamics simulations of B-type cytochrome c oxidase with the Amber force field. Data in Brief, 2016, 8, 1209-1214.	0.5	13
103	Stereoelectronic effects in stabilizing protein–N-glycan interactions revealed by experiment and machine learning. Nature Chemistry, 2021, 13, 480-487.	6.6	13
104	Local density of states calculated with the Xα scattered wave method for some clusters of silver atoms. Surface Science, 1977, 69, 714-720.	0.8	12
105	Electronic Structure Calculations: Density Functional Methods for Spin Polarization, Charge Transfer, and Solvent Effects in Transition Metal Complexes. ACS Symposium Series, 1998, , 179-196.	0.5	12
106	Mössbauer properties of the diferric cluster and the differential iron(ii)-binding affinity of the iron sites in protein R2 of class la Escherichia coli ribonucleotide reductase: a DFT/electrostatics study. Dalton Transactions, 2011, 40, 11164.	1.6	12
107	Coupled transport of electrons and protons in a bacterial cytochromecoxidase—DFT calculated properties compared to structures and spectroscopies. Physical Chemistry Chemical Physics, 2020, 22, 26652-26668.	1.3	12
108	Xα scattered wave calculations of the ionisation energies of N3P3F6 and N4P4F8. Chemical Physics Letters, 1977, 47, 265-268.	1.2	11

#	Article	IF	CITATIONS
109	Density functional and electrostatics study of oxidized and reduced ribonucleotide reductase; comparisons with methane monooxygenase. Journal of Biological Inorganic Chemistry, 2002, 7, 799-809.	1.1	11
110	The Mössbauer Parameters of the Proximal Cluster of Membrane-Bound Hydrogenase Revisited: A Density Functional Theory Study. Journal of Chemical Theory and Computation, 2016, 12, 174-187.	2.3	11
111	A Water Dimer Shift Activates a Proton Pumping Pathway in the P _{R} → F Transition of <i>ba</i> _{<i>3</i>} Cytochrome <i>c</i> Oxidase. Inorganic Chemistry, 2018, 57, 1048-1059.	1.9	11
112	DFT Fe _{a3} –O/O–O Vibrational Frequency Calculations over Catalytic Reaction Cycle States in the Dinuclear Center of Cytochrome <i>c</i> Oxidase. Inorganic Chemistry, 2019, 58, 13933-13944.	1.9	11
113	Multiple reactive immunization towards the hydrolysis of organophosphorus nerve agents: hapten design and synthesis. Bioorganic and Medicinal Chemistry, 2001, 9, 3185-3195.	1.4	10
114	A Water Molecule Residing in the Fea33+··CuB2+Dinuclear Center of the Resting Oxidized as-Isolated CytochromecOxidase: A Density Functional Study. Inorganic Chemistry, 2020, 59, 8906-8915.	1.9	10
115	Temperature-Dependent Behavior of Protein-Chromophore Interactions: A Theoretical Study of a Blue Fluorescent Antibody. ChemPhysChem, 2003, 4, 848-855.	1.0	5
116	Mapping elusive electron density. Nature Chemical Biology, 2016, 12, 391-392.	3.9	5
117	lonization energies and electronic structure of N3P3Cl6 as determined by UV photoelectron spectroscopy and the Xα scattered wave method. Chemical Physics Letters, 1978, 58, 252-258.	1.2	4
118	Correction to Density Functional Theory Calculations on Mössbauer Parameters of Nonheme Iron Nitrosyls. Inorganic Chemistry, 2011, 50, 4221-4221.	1.9	4
119	The cytochrome b lysine 329 residue is critical for ubihydroquinone oxidation and proton release at the Qo site of bacterial cytochrome bc1. Biochimica Et Biophysica Acta - Bioenergetics, 2019, 1860, 167-179.	0.5	4
120	Fe(CO)4XXX radical anion: theoretical study of the electronic structure and magnetic properties. Computational and Theoretical Chemistry, 1991, 226, 251-263.	1.5	3
121	EXAFS simulation refinement based on broken-symmetry DFT geometries for the Mn(<scp>iv</scp>)–Fe(<scp>iii</scp>) center of class I RNR from Chlamydia trachomatis. Dalton Transactions, 2014, 43, 576-583.	1.6	3
122	Modern Computational Approaches to Modeling Polynuclear Transition Metal Complexes. , 2000, , 19-47.		2
123	Mössbauer Property Calculations on Fea33+â^™â^™â^™H2Oâ^™â^™â^™CuB2+ Dinuclear Center Models of the Oxidized asâ€Isolated Cytochrome c Oxidase. ChemPhysChem, 2022, , .	Resting 1.0	2
124	Density functional calculations of redox potentials for FeS clusters including solvation effects. Journal of Inorganic Biochemistry, 1993, 51, 449.	1.5	1
125	Analysis of isotropic hyperfine parameters for mononuclear, dinuclear and polynuclear FEî—,S clusters Journal of Inorganic Biochemistry, 1993, 51, 456.	1.5	1
126	Copper(I)-Catalyzed Synthesis of Azoles. DFT Study Predicts Unprecedented Reactivity and Intermediates ChemInform, 2005, 36, no.	0.1	1

#	Article	IF	CITATIONS
127	Fe4S4 clusters as small molecule catalysts. Nature Catalysis, 2018, 1, 383-384.	16.1	1
128	Local Density Functional Approaches to Spin Coupling in Transition Metal Clusters. , 1991, , 109-123.		1
129	Quantum Chemical Studies of Intermediates and Reaction Pathways in Selected Enzymes and Catalytic Synthetic Systems. ChemInform, 2004, 35, no.	0.1	0
130	3. From the quantum chemistry of iron-sulfur clusters to redox energetics and reaction pathways in metalloenzymes. , 2017, , 21-76.		0